Journal of Mechanical Science and Technology (KSME Int. J.), Vol. 20, No. 12, pp. 2147~2158, 2006 2147

Dispersion-Based Continuous Wavelet Transform for the Analysis of Elastic Waves

Kyung Ho Sun
School of Mechanical and Aerospace Engineering and National Creative Research Initiatives Center for Multiscale Design, Seoul National University, Shinlim-Dong, San 56-1, Kwanak-Gu, Seoul 151-742, Korea
Jin-Chul Hong
Test Team 5, Test Center, Research and Development Division for Hyundai Motor Company and Kia Motors Corporation, 772-1, Jangduk-Dong, Whasung-Si, Gyunggi 445-706, Korea
Yoon Young Kim*
School of Mechanical and Aerospace Engineering and National Creative Research Initiatives Center for Multiscale Design, Seoul National University, Shinlim-Dong, San 56-1, Kwanak-Gu, Seoul 151-742, Korea

The continuous wavelet transform (CWT) has a frequency-adaptive time-frequency tiling property, which makes it popular for the analysis of dispersive elastic wave signals. However, because the time-frequency tiling of CWT is not signal-dependent, it still has some limitations in the analysis of elastic waves with spectral components that are dispersed rapidly in time. The objective of this paper is to introduce an advanced time-frequency analysis method, called the dispersion-based continuous wavelet transform (D-CWT) whose time-frequency tiling is adaptively varied according to the dispersion relation of the waves to be analyzed. In the D-CWT method, time-frequency tiling can have frequency-adaptive characteristics like CWT and adaptively rotate in the time-frequency plane depending on the local wave dispersion. Therefore, D-CWT provides higher time-frequency localization than the conventional CWT. In this work, D-CWT method is applied to the analysis of dispersive elastic waves measured in waveguide experiments and an efficient procedure to extract information on the dispersion relation hidden in a wave signal is presented. In addition, the ridge property of the present transform is investigated theoretically to show its effectiveness in analyzing highly time-varying signals. Numerical simulations and experimental results are presented to show the effectiveness of the present method.

Key Words : Elastic Wave, Dispersion, Continuous Wavelet Transform (CWT), Dispersion-Based Continuous Wavelet Transform (D-CWT), Ridge Analysis

* Corresponding Author,
E-mail : yykim@snu.ac.kr
TEL : +82-2-880-7154; **FAX** : +82-2-872-1513
School of Mechanical and Aerospace Engineering and National Creative Research Initiatives Center for Multiscale Design, Seoul National University, Shinlim-Dong, San 56-1, Kwanak-Gu, Seoul 151-742, Korea.
(Manuscript **Received** May 15, 2006; **Revised** August 30, 2006)

1. Introduction

As an alternative to the Fourier-based method, time-frequency analysis methods have received much attention in various areas of engineering. In particular, the analysis of highly time-varying signals such as dispersive wave signals in an elastic medium is a crucial application of time-frequency

analysis (Önsay and Haddow, 1994 ; Niethammer et al., 2001 ; Lemistre and Balageas, 2001 ; Lanza di Scalea and McNamara, 2004). Typical methods for time-frequency analysis include the short-time Fourier transform (STFT) (Gabor, 1946), the continuous wavelet transform (CWT) (Daubechies, 1992 ; Mallat, 1998), and the Wigner-Ville Distribution (WVD) (Wigner, 1932). Each method has its own advantages and disadvantages so that depending on the signal to be analyzed, one method performs much better than another.

Although these methods can be used for the analysis of dispersive waves, they often have difficulties when signals are (highly) dispersive. The time-frequency resolution by STFT is independent of the location in the time-frequency plane so it may be inappropriate for the analysis of a dispersive wave whose spectral components vary rapidly in time. CWT using frequency-adaptive time-frequency resolution can be more useful than STFT in the analysis of wave signals but is effective only for those signals of hyperbolic time-frequency characteristics (Mallat, 1998 ; Kim and Kim, 2001). WVD has excellent time-frequency resolution, but the smoothing of WVD is necessary to eliminate cross-term effects. To overcome the limitations of conventional time-frequency analysis methods, various modifications of STFT and CWT such as the optimal windowing (Jones and Park, 1990 ; Sun and Bao, 1996 ; Jones and Boashash, 1992 ; Hong and Kim, 2004) or adaptive ideas (Mallat and Zhang, 1993 ; Auger and Flandrin, 1995 ; Mann and Haykin, 1995 ; Baraniuk and Jones, 1996 ; Angrisani and D'Arco, 2002) have been developed. Recently, Hong et al. (2005) developed the dispersion-based STFT (D-STFT) having adaptive time-frequency tilings in order to analyze a certain class of dispersive waves.

By extending the idea used in (Hong et al., 2005) for STFT, we aim to develop an adaptive time-frequency CWT-based method, called the dispersion-based continuous wavelet transform (D-CWT). The time-frequency tiling of D-CWT is adaptively rotated with respect to the dispersion characteristics of the wave to be analyzed. Thus it can better represent the local variations of dispersive waves than CWT.

To show the effectiveness of the proposed adaptive method, the ridge property of D-CWT is investigated theoretically by using the stationary phase method (Delprat et al., 1992) and compared with that of the standard CWT. To apply the developed D-CWT method to wave signals whose dispersion relations are not known, we suggest an iterative procedure to estimate these relations. The effectiveness of D-CWT is checked by numerical and experimental studies.

2. Dispersion-Based Continuous Wavelet Transform

We define the dispersion-based continuous wavelet transform, and introduce the procedure to estimate the dispersion relations of wave signals to be analyzed. Finally, ridge property of the present transform is investigated by the stationary phase method.

2.1 Dispersion-based CWT

In this section, CWT is defined, because the dispersion-based CWT (D-CWT) is comparable with the conventional CWT. For a square-integrable function $f(t)$, its continuous wavelet transform Wf is defined as (Daubechies, 1992 ; Mallat, 1998)

$$Wf(u,s)=\int_{-\infty}^{\infty} f(t)\,\bar{\psi}_{u,s}(t)\,dt \tag{1a}$$

$$\psi_{u,s}(t)=\frac{1}{\sqrt{s}}\psi\left(\frac{t-u}{s}\right) \tag{1b}$$

where $\bar{\psi}$ denotes the complex conjugate of ψ and the function $\psi_{u,s}(t)$ is obtained by scaling $\psi(t)$ by the scaling parameter s and translating it by the translation parameter u.

The function $\Psi(t)$ is called a mother wavelet satisfying the admissibility condition

$$\int_{-\infty}^{\infty}\frac{|\hat{\psi}(\omega)|^2}{|\omega|}d\omega<\infty \tag{2}$$

where $\hat{\psi}(\omega)$ is the Fourier transform of $\psi(t)$.

The existence of the integral in Eq. (2) requires that

$$\hat{\psi}(0)=0,\ \text{i.e.}\ \int_{-\infty}^{\infty}\psi(t)\,dt=0 \tag{3}$$

In the present work, we consider only the Gabor wavelet among analytic wavelets. The Gabor wavelet has the smallest time-frequency box and its shape can be adjusted to have a desired time support. The Gabor wavelet is a complex-valued modulated Gaussian function, defined as

$$\psi(t)=2^{i\eta t}g(t) \tag{4a}$$

$$g(t)=\frac{1}{(\sigma^2\pi)^{1/4}}e^{-t^2/2\sigma^2} \tag{4b}$$

where η is the center frequency and σ is a measure of the spread of $\Psi(t)$.

The dispersion-based CWT, D-CWT, is defined by using a basis function that includes a new parameter, d:

$$W_D f(u,s)=\int_{-\infty}^{\infty} f(t)\,\bar{\psi}_{u,s,d}(t)\,dt \tag{5a}$$

$$\psi_{u,s,d}(t)=\frac{1}{\sqrt{s}}\psi\left(\frac{t-u}{s}\right)*(-id)^{-1/2}e^{i(t^2/2d)} \tag{5b}$$

where the symbol $(*)$ in Eq. (5b) denotes the convolution operator, and the parameter d determines the amount of rotation of the time-frequency box at $(u,\xi=\eta/s)$,

$$d=d(u,\xi)=\frac{\Delta u}{\Delta\xi} \tag{6}$$

The physical meaning of Eq. 5(b) can be clearly revealed in the frequency domain, as Eq. (5b) can be expressed as

$$\begin{aligned}\hat{\psi}_{u,s,d}(\omega)&=\sqrt{s}\,\hat{g}(s\omega-\eta)\,e^{-iu\omega}\cdot e^{-i\frac{d}{2}\omega^2}\\&=\sqrt{s}\,\hat{g}(s\omega-\eta)\,e^{-i\left(u\omega+\frac{d}{2}\omega^2\right)}\end{aligned} \tag{7}$$

where $\hat{g}(\omega)$ is the Fourier transform of the Gaussian window $g(t)$. Therefore, the group delay of the basis function of Eq. (5b) in the time-frequency plane is given by

$$\begin{aligned}\tau(\omega)&=\frac{d}{d\omega}\left[u\omega+\frac{d(u,\xi)}{2}\omega^2\right]\\&=u+d(u,\xi)\,\omega\end{aligned} \tag{8}$$

Equation (8) means that the time-frequency box of D-CWT can be obtained by rotating the time-frequency box of CWT by using the parameter $d(u,\xi)$. Figures 1(a) and 1(b) show a comparison of the time-frequency tilings of CWT and D-CWT, respectively. If each parameter d is chosen with respect to the local wave dispersion, the dispersion-based time-frequency tiling in Fig. 1(b) is obtained by adaptively rotating or shearing each of the analysis atoms in the time-frequency plane with respect to the wave dispersion relation.

To determine the rotating parameter $d(u,\xi)$, we may consider a uniformly sampled time-frequency location (u_i,ξ_j) as shown in Fig. 2 (where

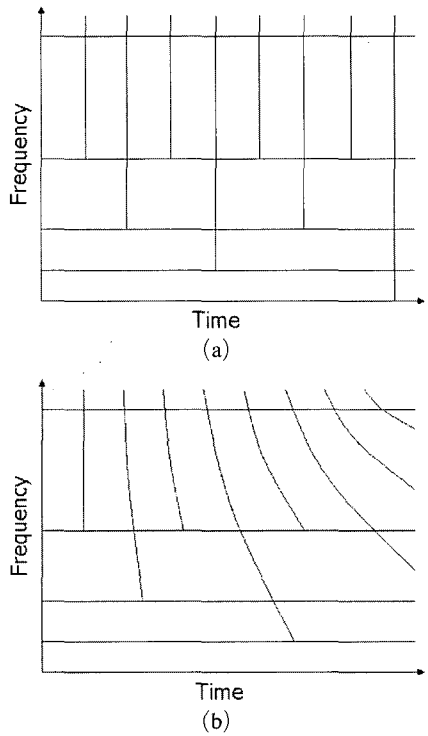

Fig. 1 A comparison of time-frequency tilings. (a) Continuous wavelet transform, (b) dispersion-based continuous wavelet transform

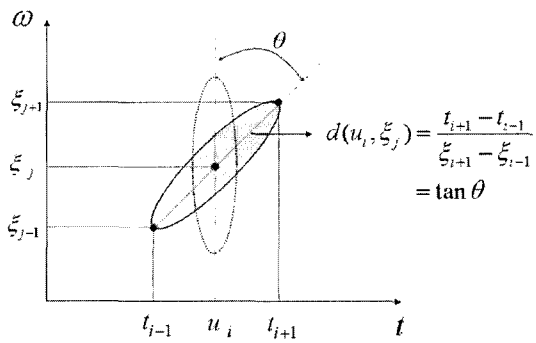

Fig. 2 The determination of the rotating parameter $d(u_i,\xi_j)$ for the given dispersion relation

u_i $(i=1,2,\cdots,m)$ are the sampled times, and ξ $(j=1,2,\cdots,n)$ are the frequencies of interest). If the dispersion relation is known or estimated, the group velocity C_g can be calculated. If a spectral component corresponding to ξ_j is measured at $t=u_i$ (assumed to be incident at $t=0$), then the traveling distance of the component can be expressed as

$$D=C_g(\xi_j)\cdot u_i \tag{9}$$

Let t_{i-1} and t_{i+1} be the arrival times of the neighboring spectral components belonging to ξ_{j-1} and ξ_{j+1}. Then, one can write

$$t_{i-1}=\frac{D}{C_g(\xi_{j-1})},\quad t_{i+1}=\frac{D}{C_g(\xi_{j+1})} \tag{10}$$

By using Eqs. (6) and (10), the rotating parameter $d(u_i,\xi_j)$ can be calculated as

$$d(u_i,\xi_i)=\frac{\Delta t}{\Delta\omega}=\frac{t_{i+1}-t_{i-1}}{\xi_{j+1}-\xi_{j-1}}=\frac{\dfrac{D}{C_g(\xi_{i+1})}-\dfrac{D}{C_g(\xi_{i-1})}}{\xi_{j+1}-\xi_{j-1}} \tag{11}$$

Because the rotating parameter $d(u_i,\xi_j)$ in Eq. (11) is linked to the local wave dispersion in the time-frequency location (u_i,ξ_j), the resulting time-frequency tiling will be suitable for the analysis of dispersive elastic wave signals.

2.2 Estimation of the dispersion relation for D-CWT

To use the dispersion-based CWT, the dispersion relation of wave signals to be analyzed must be known in advance. However, in general, the dispersion relation is not known in actual situations. Therefore, a procedure to estimate the dispersion relations from experimental wave data is needed. In this work, we present a dispersion relation estimation procedure.

The proposed strategy applies an iterative estimation scheme, in which D-CWT estimates the dispersion relation iteratively by using the initial dispersion relation determined by the standard CWT. The estimation procedure is schematically described in Fig. 3. Note that the dispersion relation or the frequency-dependent group velocity, $C_g(\omega)$, can be determined from the traveling

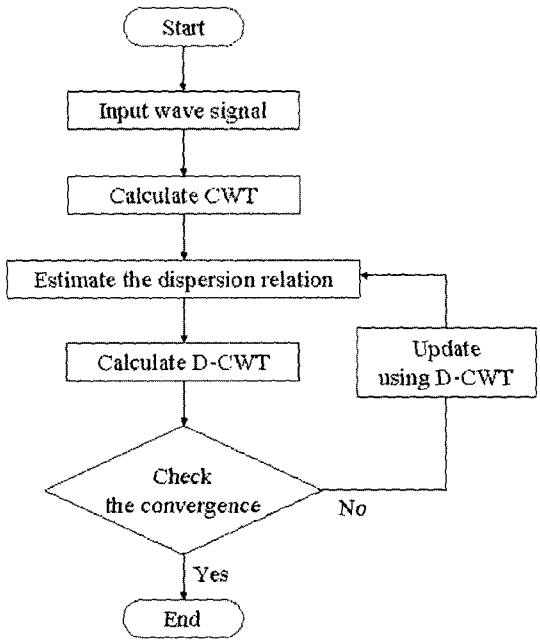

Fig. 3 Proposed procedure for estimation of the dispersion relation

distance and the arrival time of the wave signals which can be extracted by ridge analysis. After finding the initial group velocity by the standard CWT, it is used in D-CWT. Then, the group velocity is updated from the resulting D-CWT. D-CWT is repeated until the estimated group velocity satisfies the convergence criterion $R(k)$ for a prescribed small value ε,

$$R(k)=\frac{\sum_j |C_g(\xi_j)_{k+1}-C_g(\xi_j)_k|}{\sum_j |C_g(\xi_j)_k|}<\varepsilon \tag{12}$$

where j denotes the index of the considered frequency ξ and k is the number of iterations. The converged group velocity C_g is used to estimate the rotating parameter $d(u_i,\xi_j)$ by Eq. (11).

2.3 Ridge property of D-CWT

To show the effectiveness of D-CWT, we investigate its ridge property theoretically by using the stationary phase method (Delprat et al., 1992). For the subsequent analysis, the signal $f(t)$ is assumed to take the following analytic form:

$$f(t)=A_s(t)\,e^{i\phi_s(t)}\quad (A_s(t)\geq 0) \tag{13a}$$

$$\hat{f}(\omega)=\hat{A}_s(\omega)\,e^{i\hat{\phi}_s(\omega)} \tag{13b}$$

where $A_s(t)$ and $\phi_s(t)$ are a time-varying amplitude and phase of $f(t)$, respectively, and the symbol $(\hat{\ })$ denotes the Fourier transform. To evaluate $W_D f(u,s)$, we used the Fourier-transformed form of the basis function of D-CWT defined as Eq. (5b):

$$\hat{\psi}_{u,s}(\omega) = \sqrt{s}\,\hat{g}(s\omega-\eta)\,e^{-iu\omega} \tag{14a}$$

$$\begin{aligned}\hat{\psi}_{u,s,d}(\omega) &= \hat{\psi}_{u,s}(\omega)\,e^{-i\frac{d}{2}\omega^2} \\ &= \sqrt{s}\,\hat{g}(s\omega-\eta)\,d^{-i\hat{\phi}_{g_d}(\omega)}\end{aligned} \tag{14b}$$

where $\hat{\phi}_{g_d}$ denotes $u\omega+1/2\,d\omega^2$ and $\hat{g}(\omega)$ is $(4\pi)^{1/4}e^{-\omega^2/2}$. Then, D-CWT of $f(t)$, $W_D f(u,s)$ is expressed as

$$\begin{aligned}W_D f(u,s) &= \int_{-\infty}^{\infty} f(t)\,\bar{\psi}_{u,s,d}(t)\,dt \\ &= \frac{1}{2\pi}\int_{-\infty}^{\infty}\hat{f}(\omega)\,\hat{\bar{\psi}}_{u,s,d}(\omega)\,d\omega \\ &= \frac{\sqrt{s}}{2\pi}\int_{-\infty}^{\infty}\hat{A}_s(\omega)\,\hat{g}(s\omega-\eta)\,e^{i\Phi(\omega)}d\omega\end{aligned} \tag{15a}$$

$$\begin{aligned}\Phi(\omega) &= \hat{\phi}_s(\omega)+\hat{\phi}_{g_d}(\omega) \\ &= \hat{\phi}_s(\omega)+u\omega+\frac{1}{2}d(u,\omega)\,\omega^2\end{aligned} \tag{15b}$$

In the neighborhood of a stationary phase point or a ridge point $\omega=\xi(=\eta/s)$ where $\Phi'(\omega)|_{\omega=\xi}=0$ is met, the phase $\Phi(\omega)$ can be approximated by a second-order Taylor series as follows

$$\begin{aligned}\Phi(\omega) &\simeq \Phi(\xi)+(\omega-\xi)\,\Phi'(\xi)+\frac{1}{2}(\omega-\xi)^2\Phi''(\xi) \\ &= \Phi(\xi)+\frac{1}{2}(\omega-\xi)^2\Phi''(\xi)\end{aligned} \tag{16}$$

Under these hypotheses, D-CWT is expressed in the (u,ξ) plane as

$$\begin{aligned}W_D f(u,\xi) &\simeq \frac{\sqrt{s}}{2\pi}\int_{-\infty}^{\infty}\hat{A}_s(\xi)\,\hat{\bar{g}}(s\omega-\eta)\,e^{i\left(\Phi(\xi)+\frac{1}{2}(\omega-\xi)^2\Phi''(\xi)\right)}d\omega \\ &\simeq \frac{a\hat{A}_s(\xi)}{\sqrt{s^2-i\Phi''(\xi)}}e^{i\Phi(\xi)}e^{\left(\frac{is^2\Phi''(\xi)}{2(s^2-i\Phi''(\xi))}\right)}\end{aligned} \tag{17}$$

where a is $\sqrt{s}\,\pi^{-3/4}$. From the transform result of Eq. (17), the modulus of D-CWT, $M_D(u,\xi)$ and its phase $\Psi_D(u,\xi)$ in the ridge (u,ξ) are expressed as

$$M_D(u,\xi) \simeq \frac{a\hat{A}_s(\xi)}{[s^4+\Phi''^2(\xi)]^{1/4}}\exp\left(\frac{-\xi^2s^2\Phi''^2(\xi)}{2(s^4+\Phi''^2(\xi))}\right) \tag{18a}$$

$$\Psi_D(u,\xi) \simeq \Phi(\xi)+\frac{1}{2}\tan^{-1}\left(\frac{\Phi''(\xi)}{s^2}\right)+\frac{\xi^2s^4\Phi''(\xi)}{2(s^4+\Phi''^2(\xi))} \tag{18b}$$

For highly time-varying signals such as dispersive elastic waves, the second derivative of the phase $\hat{\phi}_s''(\omega)$ can not be neglected because it relates to the local time-varying patterns, namely, the rotation property of the ridges in the time-frequency plane. Thus, if the dispersion rate d is chosen to match well with $\hat{\phi}_s''(\omega)$ of the analyzed signal in the ridges, the second derivative term of the phase in Eq. (15b) will vanish:

$$\Phi''(\omega)|_{\omega=\xi}=\hat{\phi}_s''(\omega)|_{\omega=\xi}+d|_{\omega=\xi}\simeq 0 \tag{19}$$

As a result, with condition of Eq. (19), D-CWT can trace well the time-varying pattern of the analyzed signals with the selected dispersion rate d. Under this condition, the modulus and phase of D-CWT can be reduced to

$$M_D(u,\xi) \simeq \frac{a\hat{A}_s(\xi)}{s} \tag{20a}$$

$$\Psi_D(u,\xi) \simeq \hat{\phi}_s(\xi)+u\xi+\frac{1}{2}d(u,\xi)\,\xi^2 \tag{20b}$$

If the dispersion rate is not used, D-CWT is exactly equal to the standard CWT. Thus, the modulus $M(u,\xi)$ of CWT is given by

$$M(u,\xi) \simeq \frac{a\hat{A}_s(\xi)}{[s^4+\hat{\phi}_s''^2(\xi)]^{1/4}}\exp\left(\frac{-\xi^2s^2\hat{\phi}_s''^2(\xi)}{2(s^4+\hat{\phi}_s''^2(\xi))}\right) \tag{21}$$

Compared with Eqs. (20a) and (21), the modulus calculated by D-CWT is larger than that by CWT. Consequently, D-CWT can capture the local variation of the signal more accurately by using the dispersion rate and can provide more localized time-frequency analysis results.

3. Numerical Investigation

In this section, we introduce the generation of the wave signals for numerical tests, and then estimate the dispersion relation of the simulated signals by the proposed method.

3.1 Wave signal generation for numerical tests

Let us assume that a frequency-modulated Gaussian pulse $s(x=0,t)\equiv s_{in}(t)$ is generated at the point $x=0$ by a transducer and propagates along a waveguide. In the frequency domain, this

pulse can be expressed as its Fourier transform,

$$S(0,\omega)\equiv S_{in}(\omega)=\int_{-\infty}^{\infty} s_{in}(t)\,e^{-j\omega t}dt \qquad (22)$$

When the propagating pulse arrivals at the point $x=x_0$, then $S_{in}(\omega)$ is shifted in phase by $e^{-jk(\omega)x_0}$, where $k(\omega)$ denotes the frequency-dependent wavenumber. If $k(\omega)$ is known, then the Fourier transform $S(x_0,\omega)$ of the pulse measured at point $x=x_0$ can be written as

$$S(x_0,\omega)=S_{in}(\omega)\,e^{-jk(\omega)x_0} \qquad (23)$$

Consequently, the time-domain signal $S(x_0,t)$ measured at point $x=x_0$ can be obtained from the inverse Fourier transform as

$$s(x_0,t)=\frac{1}{2\pi}\int_{-\infty}^{\infty}[S_{in}(\omega)]\,e^{j\omega t}d\omega \qquad (24)$$

Equation (24) is used to build the wave signals at arbitrary locations for the numerical tests.

3.2 Estimation of the dispersion relation

D-CWT is applied to flexural and longitudinal waves in a rod (with diameter=10 mm, Young's modulus E=209 GPa, and Poisson's ratio ν=0.3). The effectiveness of D-CWT is checked by examining how well the dispersion relation is estimated. In this work, the Gabor wavelet (σ=1, η=5 in Eq. (4)) called the Morlet wavelet was employed.

3.2.1 Case I: Flexural wave in a rod

Figure 4(a) shows the simulated wave pulses generated by Eq. (24), which are based on the wavenumber $k(\omega)$ or the group velocity $C_g(\omega)$ calculated by the Pochhammer Chree equation in a rod (Miklowitz, 1978; Graff, 1975). The center frequency of the simulated pulses is 30 kHz and they have traveling distances of 0.5 and 2 m, respectively. The considered mode belongs to the lowest flexural $F(1,1)$ mode in a rod (Graff, 1975).

For the application of the proposed procedure illustrated in Fig. 3, CWT was performed as can be seen Fig. 4(b). To evaluate the group velocity $C_g(\omega)$ from this CWT data, the wave arrival times $\tau(\omega)$ were extracted by the ridge analysis

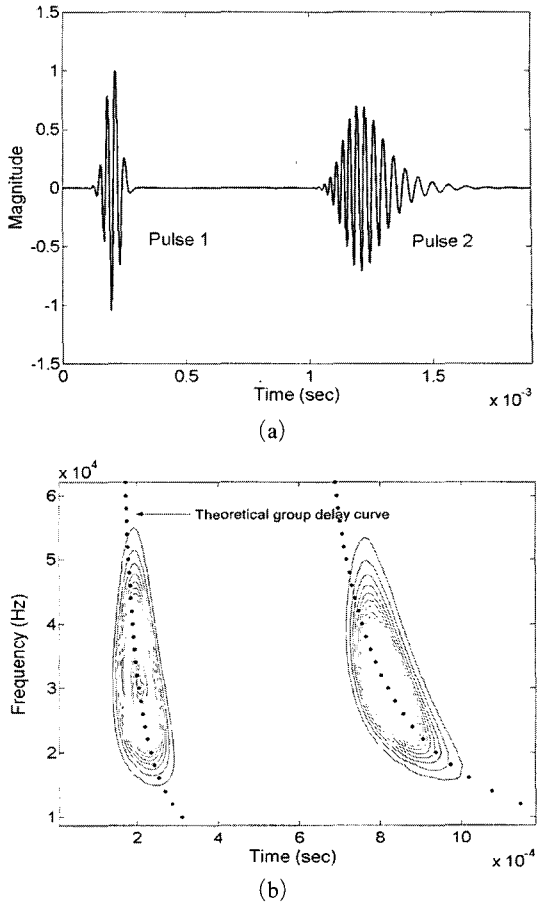

Fig. 4 CWT of a simulated flexural wave signal. (a) The simulated pulse signal, and (b) the contour plot of CWT of the simulated pulse signal

of CWT data. In calculating the group velocity $C_g(\omega)$, the following formula defined between two pulses was used

$$C_g(\omega)=\frac{D_{pulse2}-D_{pulse1}}{\tau_{pulse2}(\omega)-\tau_{pulse1}(\omega)} \qquad (25)$$

where D_{pulse} is the pulse traveling distance. The group velocity calculated using Eq. (25) was used for the first D-CWT calculation, and then D-CWT was repeated until the estimated group velocity $C_g(\omega)$ met the convergence criterion of Eq. (12) for ε=0.01. In Fig. 5(a), the estimated group velocities $C_g(\omega)$, according to the iterations, are compared with the theoretical group velocities based on the Phochhammer-Chree equa-

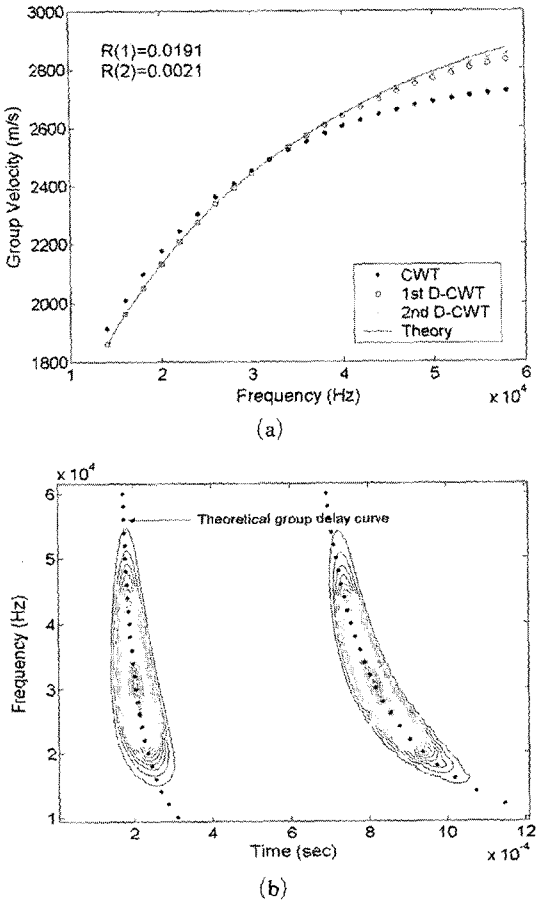

Fig. 5 D-CWT of a simulated flexural wave signal. (a) Estimation of the dispersion relation, and (b) the contour plot of D-CWT of the simulated pulse signal

tion. As can be seen in Fig. 5(a), as the number of iterations increased, the estimated group velocity approached the exact group velocity. Figure 5(b) shows a contour plot of D-CWT for the final estimated group velocity. Since the time-frequency tiling of D-CWT is based on the wave dispersion relation, it can trace the exact group delay curve.

To show the high time-frequency localization property of D-CWT, the second pulse within the simulated wave signal of Fig. 4(a) was considered. In Fig. 6, the shape and magnitude of CWT and D-CWT data at frequencies of 14, 30, and 44 kHz are compared. As can be seen in Fig. 6, D-CWT gave higher energy localization than CWT

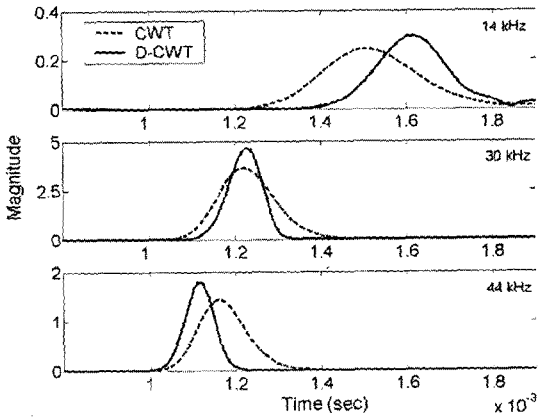

Fig. 6 The magnitudes of the second pulse shown in Fig. 4(a) for CWT and D-CWT at frequencies of 14, 30, and 44 kHz

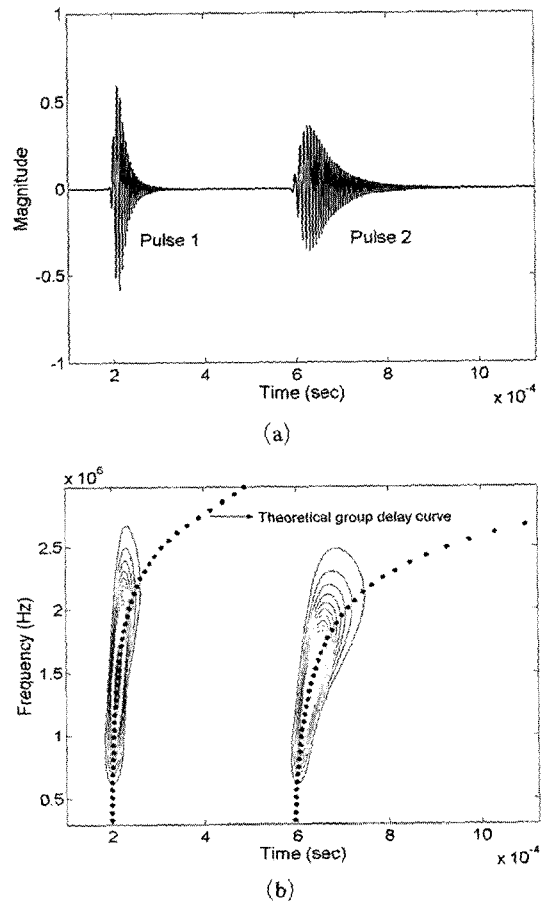

Fig. 7 CWT of a simulated longitudinal wave signal. (a) The simulated pulse signal, and (b) the contour plot of CWT of the simulated pulse signal

did. Furthermore, the magnitudes calculated using D-CWT were much larger than those calculated using CWT, as explained in the section 2.3.

3.2.2 Case II: Longitudinal wave in a rod

Figure 7(a) shows the simulated wave pulses centered at 150 kHz, which have traveling distances of 1 and 3 m. The considered mode belongs to the lowest longitudinal $L(0,1)$ mode in a rod, derived from the Pochhammer-Chree equation. As can be seen in Fig. 7(b), CWT was not suitable for the analysis of the given type of wave signals whose group delay varied quickly at high frequencies because CWT has basically a low frequency resolution at high frequencies. However, D-CWT characterized the dispersion behaviors of these wave signals more exactly than CWT did. For the given wave signal, the dispersion relation was estimated. As shown in Fig. 8(a), the group velocity estimated by D-CWT after the sixth iteration, where the convergence criterion of Eq. (12) for $\varepsilon=0.001$ was met, was very close to the exact group velocity. D-CWT using the finally estimated group velocity gave the reliable result of Fig. 8(b).

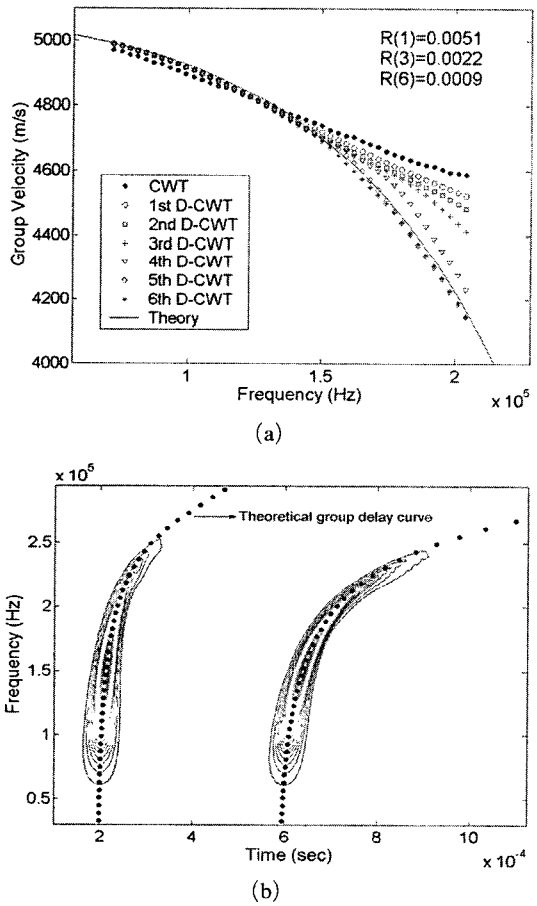

Fig. 8 D-CWT of a simulated longitudinal wave signal. (a) Estimation of the dispersion relation, (b) the contour plot of D-CWT of the simulated pulse signal

4. Experimental Verification

In this section, the performance of the dispersion-based CWT is examined experimentally, and the proposed estimation procedure of dispersion relation is applied to some dispersive elastic wave

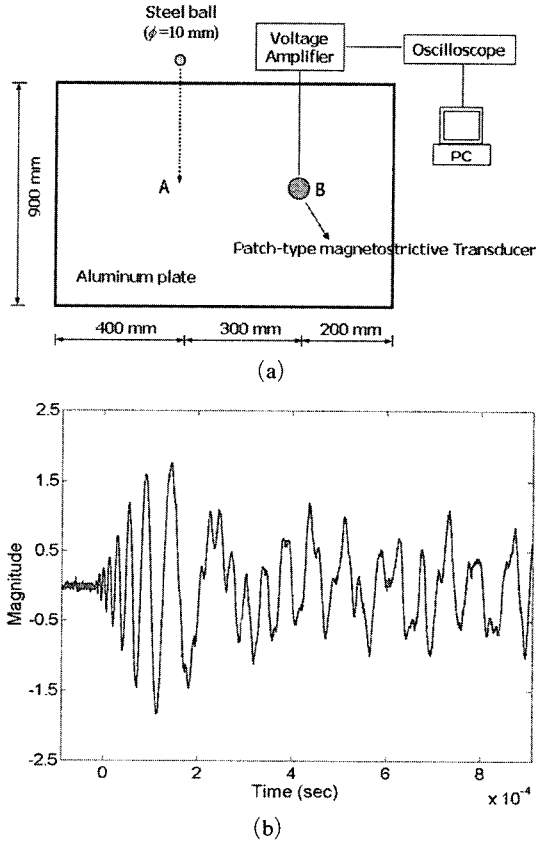

Fig. 9 (a) The experimental setup used to generate the A_0 Lamb waves in a plate, and (b) the measured A_0 Lamb wave signal

signals. In this work, we consider the fundamental modes known as the first anti-symmetric A_0 mode and the first symmetric S_0 mode of the Lamb wave propagated in a thin plate (Miklowitz, 1978 ; Graff, 1975).

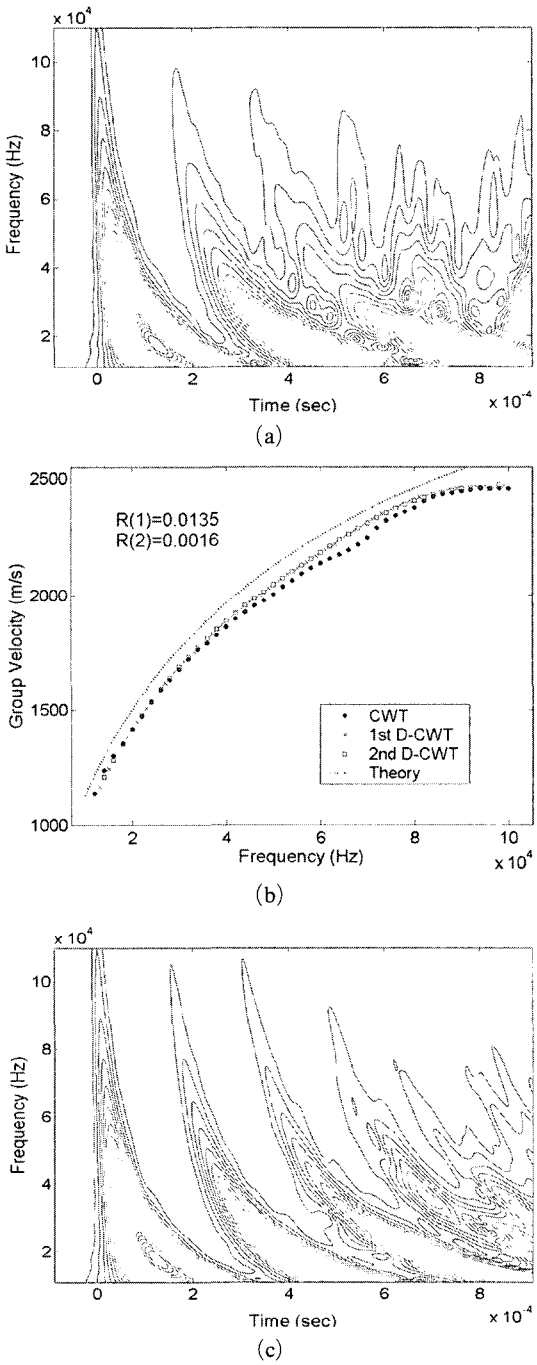

Fig. 10 CWT and D-CWT of the measured A_0 Lamb wave signal. (a) The contour plot of CWT, (b) an estimation of the dispersion relation, and (c) the contour plot of D-CWT

Figure 9(a) shows the experimental setup employed in the experiments for the A_0 Lamb wave generation in a plate. In this experimental setup, a simply supported aluminum plate with a thickness of 3 mm was excited by the impact of a steel ball dropped at the point A. The generated A_0 Lamb wave was measured at location B by using a patch-type magnetostrictive transducer (Cho et al., 2004) at a sampling frequency of 2.5 MHz.

The signal shown in Fig. 9(b) is the measured A_0 Lamb wave. Figure 10(a) shows the plot of the transformed result by CWT and the successive wave arrivals due to the wave reflections from both ends of the plate. To determine the group velocity of the measured A_0 Lamb wave, the adaptive dispersion relation estimation scheme using D-CWT was applied. The arrival times of the first and second ridges were used to estimate group velocity. Figure 10(b) shows the iteratively estimated group velocity by D-CWT and the theoretical group velocities (Graff, 1975). The finally estimated group velocity that satisfies the convergence criterion of $\varepsilon=0.01$ was utilized for D-CWT calculation of the given A_0 Lamb wave signal. Figure 10(c) shows the transformed result by D-CWT. The successive wave arrivals are clearly seen using D-CWT because of its high time-frequency localization.

D-CWT was also applied to the analysis of the S_0 Lamb wave signals in an aluminum plate shown in Fig. 11(a). Figure 11(b) shows the measured S_0 Lamb wave signal which consists of four dispersive pulses having traveling distances of 0.2, 0.68, 1.74, and 2.22 m, respectively. The transformed result from CWT is plotted in Fig. 12(a) and the history of group velocity estimation is shown in Fig. 12(b). The finally estimated group velocity where the convergence criterion of $\varepsilon=$ 0.001 was used for D-CWT calculation and the result was plotted in Fig. 12(c). As can be seen in Fig. 12(c), D-CWT traced the dispersion characteristics of the given wave signal more exactly than CWT did.

Finally, the performance of D-CWT was compared with another adaptive time-frequency analysis method reported in (Hong et al., 2005) known as the dispersion-based STFT (D-STFT). As studied in (Hong et al., 2005), D-STFT can be used effectively for the analysis of dispersive wave signals. Figures 13(a) and 13(b) show the transformed results using D-STFT for the measured A_0 Lamb wave shown in Fig. 9(b) and the S_0 Lamb wave shown in Fig. 11(b), respectively. Although D-STFT also characterizes well the dispersion behavior of the given signals, the readability in the time-frequency plane is more improved when D-CWT is applied. (Compare Figs. 10(c) and 13(a), 12(c) and 13(b))

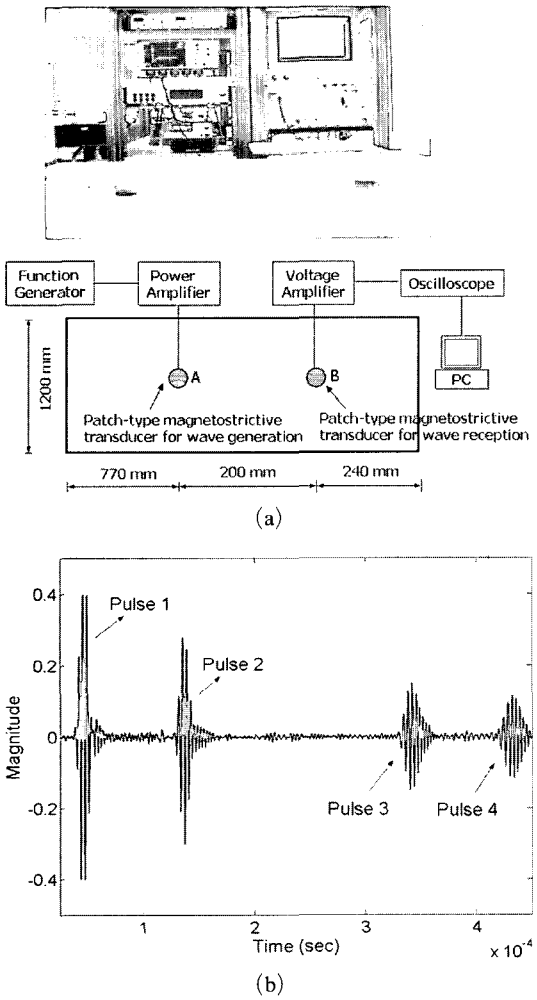

Fig. 11 (a) The experimental setup used to generate the S_0 Lamb wave in a plate, and (b) the measured S_0 Lamb wave signal

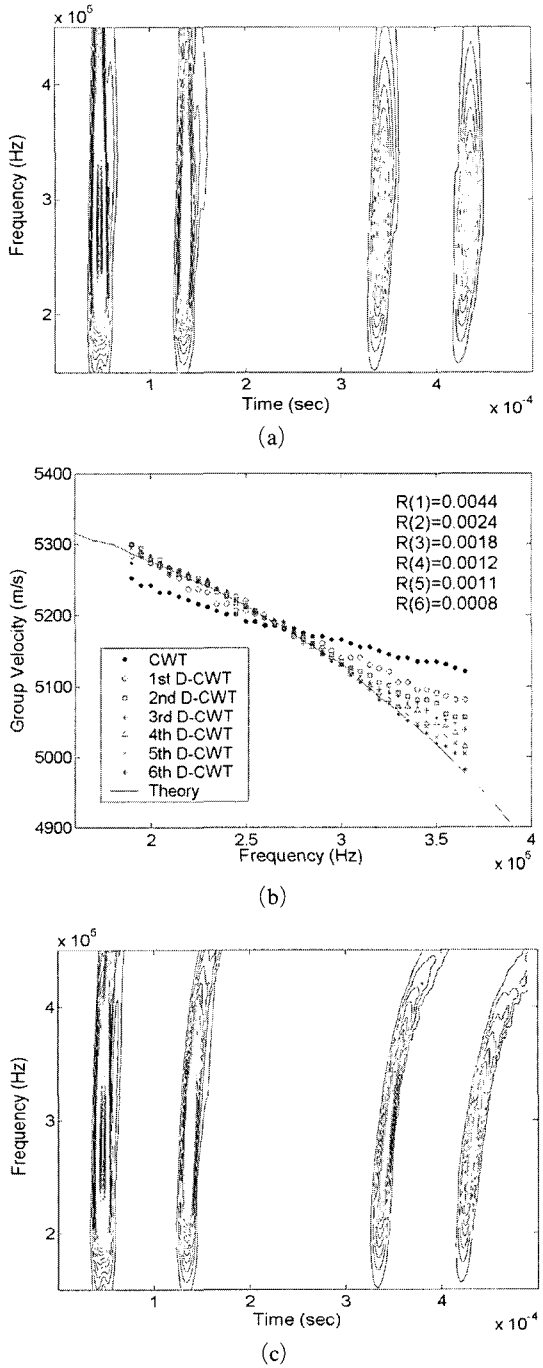

Fig. 12 CWT and D-CWT of the measured S_0 Lamb wave signal. (a) The contour plot of CWT, (b) an estimation of the dispersion relation, and (c) the contour plot of D-CWT

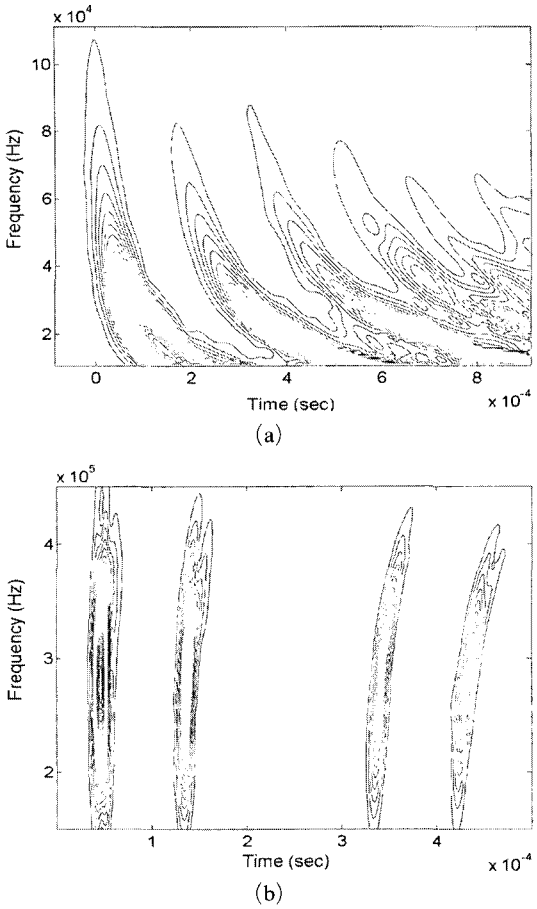

Fig. 13 D-STFT of the measured Lamb wave signal. (a) The contour plot of D-STFT of the measured A_0 Lamb wave signal, and (b) The contour plot of D-STFT of the measured S_0 Lamb wave signal

5. Conclusions

In this work, the dispersion-based continuous wavelet transform (D-CWT) was developed to analyze some class of dispersive elastic waves. To use the developed method for the analysis of signals whose dispersion is not known in advance, we developed an iterative procedure to estimate the dispersion relation. As shown from the theoretical investigation on the ridge property of D-CWT, D-CWT provided dispersion information more accurately than the standard CWT because the time-frequency tiling of D-CWT adaptively varied to the dispersion of the wave signal to be analyzed. Numerical and experimental studies confirmed the effectiveness of the present method for analyzing dispersive waves.

Acknowledgments

This research was supported by the National Creative Research Initiatives Program (Korea Science and Technology Foundation grant No. 2005-022) contracted through the Institute of Advanced Machinery and Design at Seoul National University.

References

Angrisani, L. and D'Arco, M., 2002, "A Measurement Method Based on a Modified Version of the Chirplet Transform for Instantaneous Frequency Estimation," *IEEE Transactions on Instrumentation and Measurement*, Vol. 51, pp. 704~711.

Auger, F. and Flandrin, P., 1995, "Improving the Readability of Time-Frequency and Time-Scale Representations by the Reassignment Method," *IEEE Transactions on Signal Processing*, Vol. 43, pp. 1068~1089.

Baraniuk, R. G. and Jones, D. L., 1996, "Wigner-Based Formulation of the Chirplet Transform," *IEEE Transactions on Signal Processing*, Vol. 44, pp. 3129~3135.

Cho, S. H., Sun, K. H., Lee, J. S. and Kim, Y. Y., 2004, "The Measurement of Elastic Waves in a Nonferromagnetic Plate by a Patch-Type Magnetostrictive sensor," *Proceedings of the SPIE*, Vol. 5384, pp. 120~130.

Daubechies, I., 1992, Ten Lectures on Wavelets, Philadelphia : SIAM.

Delprat, N. et al., 1992, "Asymptotic Wavelet and Gabor Analysis : Extraction of Instantaneous Frequencies," *IEEE Transactions on Information Theory*, Vol. 38, pp. 644~665.

Gabor, D., 1946, "Theory of Communication," *Proceedings of the Institute of Electrical Engineers*, Vol. 93, pp. 429~457.

Graff, K. F., 1975, Wave Motion in Elastic Solids, Ohio State Univ. Press. : Columbus.

Hong, J. -C. and Kim, Y. Y., 2004, "The De-

termination of the Optimal Gabor Wavelet Shape for the best Time-Frequency Localization Using the Entropy Concept," *Experimental Mechanics*, Vol. 44, pp. 387~395.

Hong, J. -C., Sun, K. H. and Kim, Y. Y., 2005, "Dispersion-Based Short-Time Fourier Transform Applied to Dispersive Wave Analysis," *Journal of Acoustical Society of America*, Vol. 117, pp. 2949~2960.

Jones, D. L. and Park, T. W., 1990, "A High Resolution Data-Adaptive Time-Frequency Representation," *IEEE Transactions on Acoustic, Speech, and Signal Processing*, Vol. 38, pp. 2127~2135.

Jones, G. and Boashash, B., 1992, "Window Matching in the Time-Frequency Plane and the Adaptive Spectrogram," *Proceedings of the IEEE-SP International Symposium on Time-Frequency and Time-Scale Analysis*, pp. 87~90.

Kim, Y. Y. and Kim, E. H., 2001, "Effectiveness of the Continuous Wavelet Transform in the Analysis of Some Dispersive Elastic Waves," *Journal of Acoustical Society of America*, Vol. 110, pp. 86~94.

Lanza di Scalea, F. and McNamara, J., 2004, "Measuring High-Frequency Wave Propagation in Railroad Tracks by Joint Time-Frequency Analysis," *Journal of Sound and Vibration*, Vol. 273, pp. 637~651.

Lemistre, M. and Balageas, D., 2001, "Structural Health Monitoring System Based on Diffracted Lamb Wave Analysis by Multiresolution Processing," *Smart Materials and Structures*, Vol. 10, pp. 504~511.

Mallat, S. and Zhang, Z., 1993, "Matching Pursuits with Time-Frequency Dictionaries," *IEEE* Transactions on Signal Processing, Vol. 41, pp. 3397~3415.

Mallat, S., 1998, A Wavelet Tour of Signal Processing, Academic Press : London.

Mann, S. and Haykin, S., 1995, "The Chirplet Transform : Physical Considerations," *IEEE Transactions on Signal Processing*, Vol. 43, pp. 2745~2761.

Miklowitz, J., 1978, Elastic Waves and Waveguides, North-Holland : New York.

Niethammer, M., Jacobs, L. J., Qu, J. and Jarzynski, J., 2001, "Time-Frequency Representations of Lamb Waves," *Journal of Acoustical Society of America*, Vol. 109, pp. 1841~1847.

Önsay, T. and Haddow, A. G., 1994, "Wavelet Transform Analysis of Transient Wave Propagation in a Dispersive Medium," *Journal of Acoustical Society of America*, Vol. 95, pp. 1441~1449.

Sun, X. and Bao, Z., 1996, "Adaptive Spectrogram for Time-Frequency Signal Analysis," *Proceedings of 8th IEEE Signal Processing Workshop on Statistical Signal and Array Processing*, pp. 460~463.

Wigner, E. P., 1932, "On the Quantum Correction for Thermodynamic Equilibrium," *Physics Review*, Vol. 40, pp. 749~759.